



Platinum electrodeposition in porous silicon: The influence of surface solvation effects on a chemical reaction in a nanospace

Kazuhiro Fukami^{a,*}, Ryo Koda^a, Tetsuo Sakka^a, Tomoko Urata^a, Ken-ichi Amano^a, Hikaru Takaya^b, Masaharu Nakamura^b, Yukio Ogata^a, Masahiro Kinoshita^a

^aInstitute of Advanced Energy, Kyoto University, Uji, Kyoto 611-0011, Japan

^bInstitute for Chemical Research, Kyoto University, Uji, Kyoto 611-0011, Japan

ARTICLE INFO

Article history:

Received 7 May 2012

In final form 29 May 2012

Available online 7 June 2012

ABSTRACT

A chemical reaction in a nanospace is decelerated once a diffusion-limited condition is reached due to the difficulty in supply of reactants from the bulk. We illustrate how to overcome this problem for platinum electrodeposition within nanoporous silicon electrodes. The surface-induced hydration structure of reactants is essential. We make nanopore surfaces hydrophobic by covering them with organic molecules and adopt platinum complex ions with sufficiently large sizes as reactants. Due to the resulting fact that the ions are strongly excluded from the bulk solution to the surface, the ion concentration is greatly enriched within nanopores. This enrichment accelerates the reaction.

© 2012 Elsevier B.V. All rights reserved.

1. Introduction

A chemical reaction occurring in a nanospace is an important process enabling development of novel science and technology or highly functional materials and devices. However, the control of the reaction is difficult to achieve in a conventional way using the temperature and concentration of reactants in bulk solution [1–7]. A typical problem is that the reaction in a nanospace can remarkably be decelerated due to a diffusion-limited condition reached (i.e., the difficulty in supply of reactants from the bulk through mass transfer). In modeling and understanding the reaction mechanism in a nanospace, the solvent confined by a surface or surfaces should play crucially important roles. It has been shown that the structure of ionic liquid or organic solvent near a nanosurface is substantially different from that in bulk [8–10]. Here we show that the surface-induced solvation structure of reactants has surprisingly large effects on the reaction process. By adjusting the affinity of surfaces for the solvent and the solvation properties of reactants, the reaction process can be controlled in a variety of manners, for instance, to overcome the deceleration problem mentioned above. A statistical-mechanical theory for confined molecular liquids provides a useful guide to the control that can be achieved by manipulating the affinity of electrode surfaces for water and varying the ion size.

In the present Letter, porous silicon and platinum electrodeposition are used as platforms of a nanospace and a chemical reaction, respectively. The pore diameter is ~5 nm at its maximum and ~3 nm on the average. With platinum electrodeposition, we can

visualize the past record of reaction process by investigating the density and distribution of platinum deposit within the porous structure (deposited platinum is stable against the spontaneous dissolution). In this case, the solvent is water and the reactants are platinum complex ions. The important point is that the hydration properties of reactants in the aqueous solution confined on the scale of a nanometer are substantially different from those in the bulk aqueous solution. More specifically, the surface-induced hydration structure of reactants, which has never been considered explicitly in electrochemical research, is experimentally explored by covering the nanopores with organic molecules to make their surface hydrophilic or hydrophobic and by testing different ion sizes of reactants. Theoretical analyses based on a molecular model (not a dielectric continuum model) for water are also employed. As a striking result, the physical factor that the ions are excluded from the bulk water to the surface comes into play when the surface is hydrophobic, leading to enrichment of the ion concentration within nanopores. Moreover, the degree of this enrichment is remarkably influenced by the ion size.

2. Experimental method

Nanoporous silicon electrodes were prepared by anodization of a p-Si (100) wafer (Shin-Etsu Astech Co. Ltd.). The resistivity of the silicon was 10–20 Ω cm. All chemicals purchased from Nacalai Tesque, Inc. with analytical grade were used without further purification. The anodization was performed in 22 wt.% HF ethanolic solution at current density of 2.0 mAcm⁻² for 20 min with a conventional potentio/galvanostat (Hokuto Denko, HZ-3000). The anodized area was 0.78 cm² (1 cm in diameter).

* Corresponding author.

E-mail address: fukami.kazuhiro.2u@kyoto-u.ac.jp (K. Fukami).

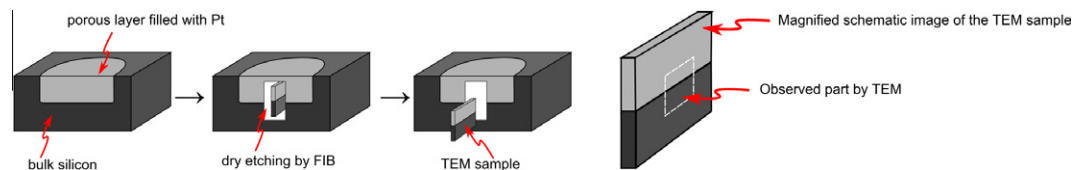


Figure 1. Schematic illustration explaining how the TEM sample was prepared and which part of the sample was considered for the observation by TEM.

After washing the as-anodized nanoporous silicon with water and ethanol, the substrate was immersed for 15 h in n-hexane containing 0.2 M propionic acid or 0.2 M methyl propiolate to cover the pore-wall surfaces with the organic molecules [11]. We note that it is better to graft almost similar molecules which show the opposite hydration properties, i.e., hydrophobic and hydrophilic, to understand the effect of surface-induced hydration structures. This is because the molecules on the pore wall strongly affect the electrochemical behavior, meaning that analyses of the electrochemical property become quite complex if one uses molecules with substantially different structures. Propionic acid and methyl propiolate form one of the best combinations for the present Letter from this point of view. The chemically-modified nanoporous silicon substrate was analyzed using a Fourier-transform infrared spectrometer (JASCO, FT/IR-460 Plus; FT-IR) with a diffuse-reflection mode. The contact angles of the porous layers were evaluated using a contact-angle measure (KSV Instruments, CAM 200).

The deposition bath was aqueous solution containing 0.1 M K_2PtCl_4 and 0.5 M NaCl. Aqueous solution containing 0.1 M K_2PtBr_4 and 0.5 M KBr was also used to examine the ion-size effect. The platinum electrodeposition was carried out cathodically at current density of $-6.4 \mu A cm^{-2}$ (the minus sign means ‘cathodic’ current density). The cross-sectional views of the platinum deposited nanoporous silicon were observed with a field-emission scanning electron microscope (FE-SEM) (JEOL, JSM-6500F; SEM) and analyzed by an energy-dispersive X-ray spectrometer (EDS) equipped in the SEM. The nanoscopic images of the cross-section were observed with a scanning transmission microscope (JEOL, JEM-2200FS; STEM). To prepare the samples for the STEM observation, the porous layers were sliced into thin films using a focused ion beam (JEOL, JIB-4500; FIB). The schematic illustration shown in Figure 1 explains how the STEM samples were prepared and which part of the sample was considered for the observation by STEM.

3. Theoretical method

It is required that a molecular model be employed for water to investigate the effects of the ion size. A water molecule is modeled as a hard sphere with diameter $d_s = 0.28$ nm in which a point dipole and a point quadrupole of tetrahedral symmetry are embedded [12]. The influence of molecular polarizability of water is included by employing the self-consistent mean field (SCMF) theory [12]. Hard spherical cations and anions with diameters d_+ and d_- , respectively, are immersed in water. The water-water and water-ion correlations are then dependent not only on the distance between centers of the particles but also on the particle orientations. We analyze the structure of electrolyte solution at an extended, uncharged (hydrophobic) or charged (hydrophilic) surface. The water-surface correlations are also dependent on the orientations of water molecules.

We employ the angle-dependent integral equation theory [12–15], a statistical-mechanical theory for molecular liquids. A macroparticle with diameter $d_M = 30d_s$ (d_s is the diameter of water molecules, 0.28 nm) mimicking an extended surface is immersed in aqueous electrolyte solution. The subscripts, ‘S’, ‘+’, ‘-’, and ‘M’ respectively, represent ‘solvent (water)’, ‘cations’, ‘anions’, and

‘macroparticle’. The Ornstein–Zernike (OZ) equation for the mixture comprising water molecules, cations, and anions can be written as [12–17]

$$\eta_{\alpha\beta}(12) = \{1/(8\pi^2)\} \sum_{\gamma} \rho_{\gamma} \int c_{\alpha\gamma}(13) \{ \eta_{\gamma\beta}(32) + c_{\gamma\beta}(32) \} d(3) \quad (1a)$$

$$\eta_{\alpha\beta}(12) = h_{\alpha\beta}(12) - c_{\alpha\beta}(12); \alpha, \beta = S, +, -, M \quad (1b)$$

where h and c are the total and direct correlation functions, respectively, (ij) represents $(r_{ij}, \Omega_i, \Omega_j)$, r_{ij} is the vector connecting the centers of particles i and j , Ω_i denotes the three Euler angles describing the orientation of particle i , $\int d(3)$ represents integration over all position and angular coordinates of particle 3, and ρ is the number density. The closure equation is expressed by [12–17]

$$c_{\alpha\beta}(12) = \int_{r_{12}}^{\infty} [h_{\alpha\beta}(12) \partial \{ w_{\alpha\beta}(12) - b_{\alpha\beta}(12) \} / \partial r'_{12}] dr'_{12} - u_{\alpha\beta}(12)/(k_B T) + b_{\alpha\beta}(12) \quad (2a)$$

$$w_{\alpha\beta}(12) = -\eta_{\alpha\beta}(12) + u_{\alpha\beta}(12)/(k_B T) \quad (2b)$$

where u is the pair potential, b is the bridge function, and $r_{12} = |\mathbf{r}_{12}|$. In the present analysis, the hypernetted-chain (HNC) approximation is employed ($b = 0$). We assume that the macroparticle is present at infinite dilution ($\rho_M \rightarrow 0$). The calculation process can then be split into two steps:

Step (i). Solve Eqs. (1 and 2) for bulk aqueous electrolyte solution. Calculate the correlation functions X_{SS} , X_{S+} , X_{S-} , X_{++} , X_{+-} , and X_{--} ($X = h, c$).

Step (ii). Solve Eqs. (1 and 2) for the macroparticle–aqueous electrolyte solution system using the correlation functions obtained in step (i) as input data. Calculate the correlation functions X_{MS} , X_{M+} , and X_{M-} ($X = h, c$).

For the numerical solution of Eqs. (1 and 2), the pair potentials and correlation functions are expanded in a basis set of rotational invariants (i.e., Wigner’s generalized spherical harmonics), and the basic equations are reformulated in terms of the projections $X_{\mu\nu}^{mnl}(r)$ occurring in the rotational-invariant expansion of X [12–17]. The expansion considered for $m, n \leq n_{\max} = 4$ gives sufficiently accurate results. The basic equations are then numerically solved using the robust, highly efficient algorithm developed by Kinoshita and coworkers [14,18]. In the numerical treatment, a sufficiently long range r_L is divided into N grid points ($r_i = i\delta r$, $i = 0, 1, \dots, N-1$; $\delta r = r_L/N$) and all of the projections are represented by their values on these points. The grid width and the number of grid points are set at $\delta r = 0.01d_s$ and $N = 4096$, respectively.

In the real porous structure, the solution is confined within pores having various sizes whose surfaces are concave. However, the analyses on the solution confined by an extended surface provide fundamental information which can readily be applied to the solution confined between two extended surfaces, between two concave surfaces, or within a nanopore in a qualitative sense. The microstructure (heterogeneity) of the surface is not taken into account in the theoretical calculation. However, it has been shown that it has no essential effects on the conclusion as long as the averaged properties of the surface-induced structure are discussed [19].

4. Results and discussion

4.1. Electrodeposition in aqueous solution of $[\text{PtCl}_4]^{2-}$

First, platinum electrodeposition was carried out in aqueous solution of $[\text{PtCl}_4]^{2-}$ using the hydrophobic and hydrophilic nanoporous silicon electrodes. Figure 2 shows images of contact angle measurements, cross-sectional SEM images, and mappings of Si and Pt by EDS using the hydrophilic and hydrophobic porous silicon electrodes. The contact angles of the chemically-modified porous silicon electrodes in Figure 2a and b are 78° and 122° , respectively. The modifications of porous silicon were also charac-

terized by FT-IR measurements (see [Supplementary content](#)). As shown in Figure 2c, e, and g, platinum deposits are mainly observed on the top of the porous silicon when the hydrophilic porous electrode is employed. On the contrary, in Figure 2d, f, and h, platinum is uniformly deposited within the porous layer by the use of the hydrophobic porous electrode.

Current density-potential (i - E) curve measurements were performed to understand the electrodeposition behavior on various surfaces (Figure 3). A platinum plate, a bare p-Si(100), and chemically-modified p-type silicon (100) substrate were used as the working electrodes. According to the i - E curves, the chemically-modified electrodes require much higher overpotential than a

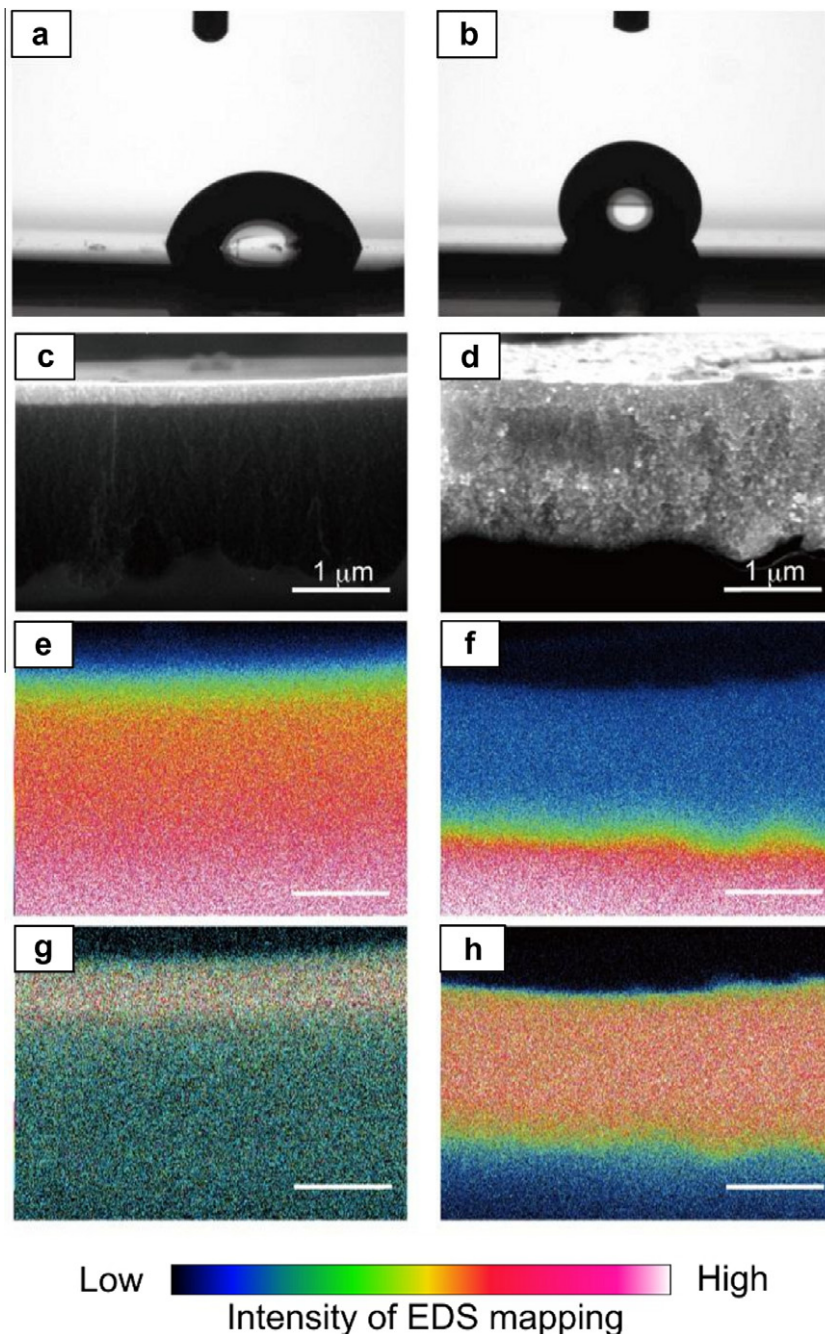


Figure 2. Strong effect of surface properties of porous silicon electrodes on platinum electrodeposition in which $[\text{PtCl}_4]^{2-}$ is used as platinum source. The electrode surfaces are hydrophilic in (a), (c), (e), and (g) whereas they are hydrophobic in (b), (d), (f), and (h). Images of contact angle measurements are shown in (a) and (b), cross-sectional SEM images in (c) and (d), EDS mappings of Si in (e) and (f), and EDS mappings of Pt in (g) and (h) after the platinum electrodeposition. The gradation bar in the bottom of the Figure indicates the relative intensity of each element detected in the mapping. A marked difference in the electrodeposition behavior is observed between (g) and (h).

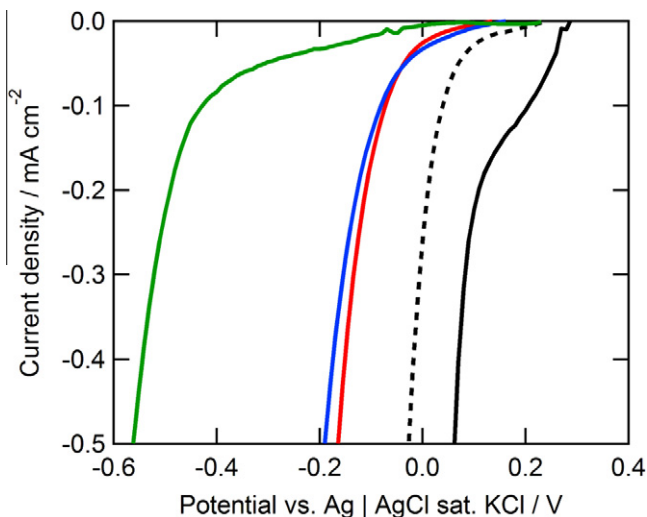


Figure 3. Current density-potential curves measured on various electrodes. The black, black-dotted, red, and blue curves were measured using a platinum plate, bare p-Si (100), propiolic acid-modified p-Si (100), and methyl propiolate-modified p-Si (100), respectively. The measurements were carried out in aqueous solution containing 0.1 M K_2PtCl_4 and 0.5 M NaCl. The green curve was also measured with a methyl propiolate-modified p-Si (100), but in an aqueous solution containing 0.1 M K_2PtBr_4 and 0.5 M KBr. The scan rate of potential was 10 mVs^{-1} .

platinum plate electrode. However, the difference in the overpotential between the propiolic acid-modified p-Si and the methyl propiolate-modified one is not large, meaning that the electrochemical properties of these electrodes are similar. The electrodeposition was carried out under a constant-current condition. Therefore, the hydrophilic and hydrophobic electrodes share the same total electric charge and duration of deposition. In addition, the current efficiency for the platinum deposition is expected to be nearly 100% because the current density is extremely small. It follows that the amounts of deposited platinum are the same for the hydrophilic and hydrophobic porous silicon electrodes but the preferential deposition sites are completely different. This, in turn, means that the difference between them in deposition behavior (Figure 2) originates solely from the surface-induced hydration structure of $[PtCl_4]^{2-}$ which is dependent on the surface properties. We have performed an additional experiment. The amount of platinum deposited on as-anodized nanoporous silicon, whose surface (it is not modified with the organic molecules) shows the highest hydrophobicity, is drastically larger as depicted in Figure 4. Because the electrochemical properties are different from those of the modified electrodes (Figure 3), one cannot compare the results in a simple way. However, it has been verified that the hydrophobic pore wall enhances the deposition reaction within the nanopores. Further, as discussed in the latter part of this Letter (see Figure 6), the electrodeposition with a different platinum complex ion exhibits the same behavior as that with $[PtCl_4]^{2-}$, i.e., platinum deposition is substantially enhanced within the hydrophobic porous layer. These results indicate that the behavior is quite general and the specific chemical properties of functional groups on the modified surface and metal ions are not relevant.

4.2. Theoretical analyses

The above result was elucidated by our statistical-mechanical theory for confined molecular liquids. Our principal concern is the normalized number-density profile of anions $g(h) = \rho(h)/\rho_-$ where h is the distance from the surface, $\rho(h)$ is the number-density profile of anions, and ρ_- is the number density of anions in the bulk: $g(h)$ represents the surface-induced hydration structure of

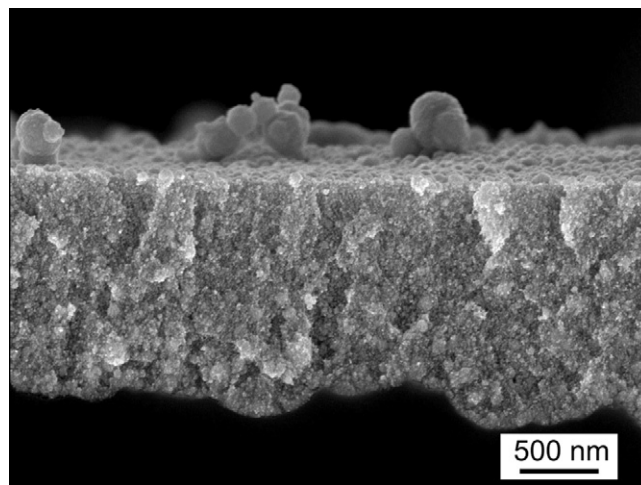


Figure 4. Cross-sectional SEM image of as-anodized nanoporous silicon after platinum electrodeposition. The condition for electrodeposition was the same as that in Figure 2, but the pore surface was not modified with organic molecules. Platinum is densely deposited within the porous layer. The pore surface is hydrogen-terminated, meaning that it is more hydrophobic than methyl propiolate.

anions and $g(h) \rightarrow 1$ as $h \rightarrow \infty$. Our experience in theoretical analyses for alkali-halide ions has shown that the profile is rather insensitive to the ion concentration in the bulk over its wide range ($<3\text{ M}$) [15]. It is far more sensitive to the ion size. It is not significantly influenced by the species of the coexisting cations. On the basis of this information, the aqueous solution is treated as water containing K_2PtCl_4 at 1 mM. The anion, $[PtCl_4]^{2-}$, is modeled as a spherical ion within which the point charge of $-2|e|$ (e is the electronic charge) is placed at the center. The point charge of K^+ placed at its center is $|e|$. The cation size d_+ is set at 0.3 nm. As the anion size d_- , 0.60 nm is adopted for $[PtCl_4]^{2-}$. The size of $[PtCl_4]^{2-}$ was approximately calculated from the molecular weight and density of K_2PtCl_4 in solid state with the tetragonal crystal structure.

First, we show $g(h)$ near a hydrophobic surface in Figure 5. Two more values, 0.65 nm and 0.70 nm, are tested for d_- to look at the size effect. The anion concentration is enriched in the immediate vicinity of the surface. The cations are highly hydrophilic due to their small size and they are preferentially hydrated in the bulk, with the result that they are depleted near the surface. Further, the concentration of K_2PtCl_4 in the bulk is very low: 1 mM. The cations have essentially no effects on the anion behavior. Of course, the local charge neutrality does not hold near the surface. Strong enrichment of $g(h)$ occurs only within the first layer of the particles ($(h-d_-/2)/d_s \sim 1$). Even in Figure 5c, $g(h)$ reduces quite rapidly as h increases, and the values of $g(h)$ are only 2.7 and 1.1 within the second ($(h-d_-/2)/d_s \sim 2$) and third ($(h-d_-/2)/d_s \sim 3$) layers, respectively. The physical interpretations of the enrichment and the great dependence on the anion size are given as follows.

(1) $d_- = 0.60\text{ nm}$

We consider system 1 where the charges of ions and the point dipole and quadrupole of water molecules are all switched to zero: A mixture of hard spheres with three different diameters (d_s , d_+ , and d_-) forms the solution. The surface is made by a hard wall. In this system, all of the allowed system configurations share the same energy and the system behavior is purely entropic in origin. The measure of the enrichment, $g(d_-/2)$, is ~ 30 . This entropic enrichment arises from 'the packing force' (see Supplementary content) [20]. We then consider system 2 where only the charges of ions are set at zero. A binary mixture of hard spheres with different diameters (d_+ and d_-), which form hydrophobic solutes, is immersed in water. $g(d_-/2)$ reaches ~ 67000 . Energetically, water

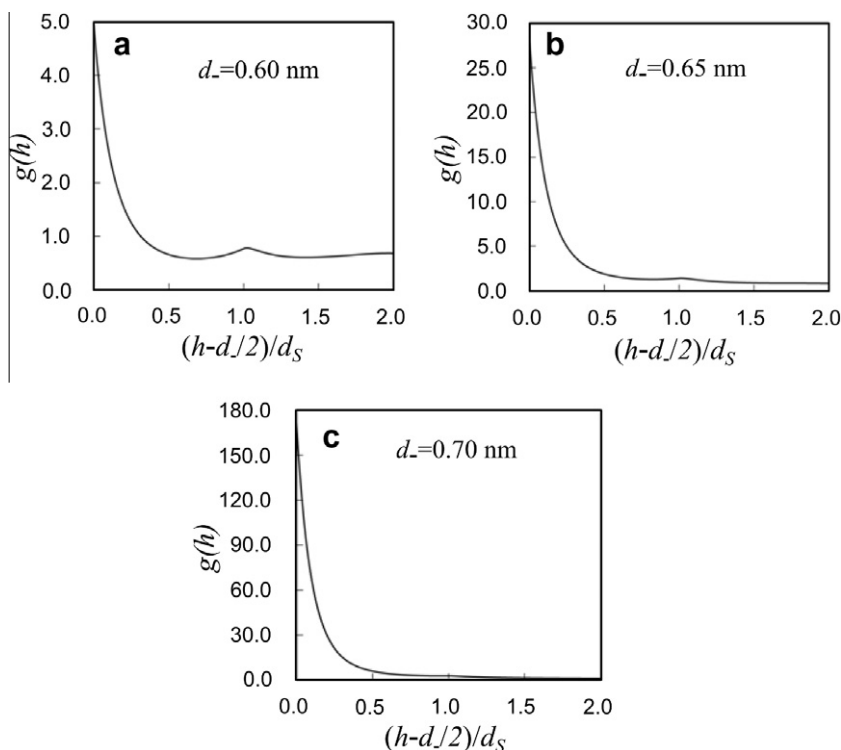


Figure 5. Remarkable effect of anion size on surface-induced hydration structure of anions: Normalized number-density profile of anions $g(h)$ near an extended hydrophobic surface for the three different values of d_- , 0.60 nm (a), 0.65 nm (b), and 0.70 nm (c). The anions in (a) and (c) correspond to $[\text{PtCl}_4]^{2-}$ and $[\text{PtBr}_4]^{2-}$, respectively. The profile exceeding 1 near the surface indicates the enrichment of anion concentration. Our experience in analyses on confined electrolyte solutions has shown the following [15]. Let us consider the solution confined between two extended surfaces. When the surface separation H is large, the solution around the center is very much like that in the bulk and $g(h)$ near each of the surfaces is close to $g(h)$ near a single surface. As H becomes smaller, the solution for all h is more influenced not only by the nearest surface but also by the other surface. When H becomes smaller than a few times of the diameter of a water molecule, $g(h)$ for all h exhibits an upward shift and the anion-size effect becomes larger. The upward shift and the enhancement of anion-size effect are more appreciable when H is smaller or the surface is concave and its curvature is larger (see 'Entropic enrichment originating from packing force' in Supplementary content). By the interplay of these physical factors, the enrichment of anion concentration and the anion-size effect become remarkable when the solution is confined within a pore having the size of a nanometer.

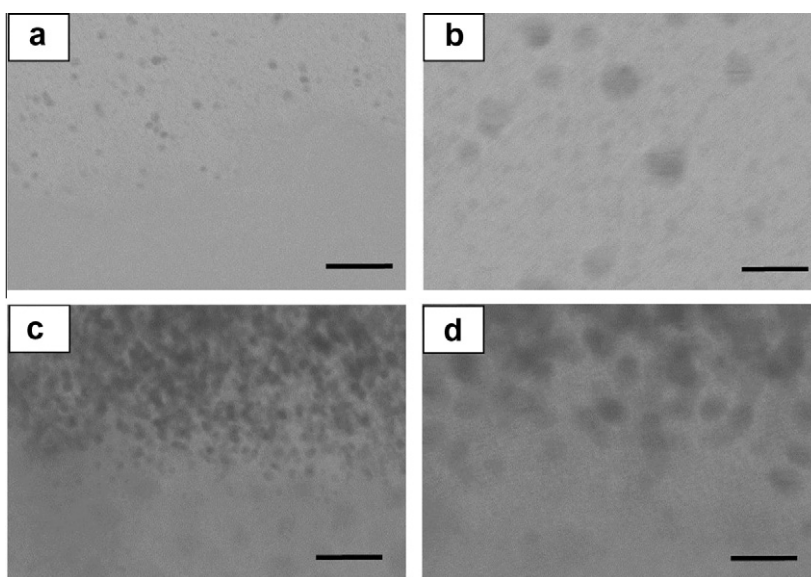


Figure 6. Substantially large increase in the density of platinum nanoparticles in the case where $[\text{PtBr}_4]^{2-}$ is used as platinum source: Cross-sectional STEM images of the hydrophobic porous silicon after the electrodeposition of platinum. The samples of (a, b) and (c, d) are deposited in deposition baths containing $[\text{PtCl}_4]^{2-}$ and $[\text{PtBr}_4]^{2-}$, respectively. The images (b, d) are magnified images of (a, c). The scale bars in (a, c) and (b, d) indicate 30 and 10 nm, respectively.

molecules do not want to accommodate a solute which cannot participate in the hydrogen bonding. The number of water molecules surrounding such a hydrophobic solute N_C is an important quan-

tity. N_C for the solute in contact with the surface is half of N_C for the solute in the bulk. Therefore, the solutes are strongly excluded from water to the surface, which forms those with smaller N_C .

When the charges are given to the ions (system 3: the model aqueous solution specified in the last paragraph), $g(d_-/2) \sim 5$ as observed in Figure 5a. This value is smaller than 30 in system 1, and the anions with $d_- = 0.60$ nm are rather favored by water: they are weakly hydrophilic.

(2) $d_- = 0.70$ nm

It has been found that $g(d_-/2) \sim 44$ in system 1 and $g(d_-/2) \sim 170$ in system 3 as observed in Figure 5c. The latter value is larger than the former one, and the anions with $d_- = 0.70$ nm are unfavorable for water: they are rather hydrophobic despite that the charge carried by them is as large as $-2|e|$. This property is ascribed to the large anion size.

As explained in the caption for Figure 5, the enrichment becomes larger as the pore diameter decreases. For a pore having the size of a nanometer, the anion concentration within the whole nanospace is made far higher than that in the bulk.

We repeat that $g(h)$ and $g(d_-/2)$ remain roughly constant against a change in the anion concentration in the bulk C_- . However, the number-density profile and the number density of anions near the surface *themselves* (not normalized) increase in proportion with C_- . Actually, in our experiments, the electrodeposition behavior of platinum within the hydrophobic porous layer displayed a rather abrupt change at around the $[\text{PtCl}_4]^{2-}$ concentration of ~ 10 mM. Below this concentration, the electrodeposition occurred preferentially on the top of the hydrophobic porous layer, which is indicative that the concentration of $[\text{PtCl}_4]^{2-}$ near the surface is not high enough to deposit platinum despite almost the same degree of the enrichment. It is interesting that such a threshold value exists for C_- .

We then discuss the theoretical result for a hydrophilic surface. When the surface is negatively charged (i.e., hydrophilic) as in our experiments described above, within the surface-induced layer the anions are largely depleted ($g(d_-/2) \ll 1$). The depletion becomes more remarkable as the pore diameter decreases. There are two reasons for this behavior. The first reason is that the anions are repelled from the surface through electrostatic interaction. The second one is that the number density of water molecules is higher within a nanopore and the insertion of rather hydrophobic ions into the nanopore is less allowed.

4.3. Electrodeposition in aqueous solution of $[\text{PtBr}_4]^{2-}$

Figure 5 indicates that the enrichment of anion concentration is drastically enhanced by a minor increase in the anion size. To demonstrate this size effect, the deposition experiment was carried out in the bath containing $[\text{PtBr}_4]^{2-}$. The size difference between $[\text{PtBr}_4]^{2-}$ and $[\text{PtCl}_4]^{2-}$ can be set at the double of that between Br^- and Cl^- with the result that the size of $[\text{PtBr}_4]^{2-}$ is ~ 0.7 nm which corresponds to Figure 5c [21]. Figure 6 depicts the microscopic structures of the deposited platinum in the $[\text{PtCl}_4]^{2-}$ and $[\text{PtBr}_4]^{2-}$ baths. In Figure 6a and b, platinum is deposited as nanoparticles with ~ 4 nm in diameter, which is almost the same as the diameter of the original pores of porous silicon. These are images of the interfaces between bulk silicon and the hydrophobic porous layer (Figure 2), showing that platinum complex ions were continuously supplied to the bottom and platinum electrodeposition occurred smoothly. As predicted by our theory, the deposition behavior exhibited a drastic change when platinum deposition was carried out in the $[\text{PtBr}_4]^{2-}$ bath. The density of platinum nanoparticles is obviously increased when $[\text{PtBr}_4]^{2-}$ is used as platinum source (Figure 6c and d). Strikingly, the electrochemical properties of $[\text{PtCl}_4]^{2-}$ bath are different from those of $[\text{PtBr}_4]^{2-}$ bath in the respect that the latter requires much higher overpotential than the former (see Figure 3). It follows that the deposition of $[\text{PtCl}_4]^{2-}$ would be much easier than that of $[\text{PtBr}_4]^{2-}$ from the

electrochemical viewpoint. Nevertheless, $[\text{PtBr}_4]^{2-}$ produces much higher density of platinum particles within the hydrophobic porous electrode than $[\text{PtCl}_4]^{2-}$. This result strongly suggests that in cases of nanopores the surface-induced hydration structure of platinum complex ions plays dominant roles in the reaction mechanism.

5. Concluding remarks

We have illustrated how to control a chemical reaction occurring in a nanospace for platinum electrodeposition within nanoporous silicon electrodes as an example. The surface-induced hydration structure of reactants is shown to be crucially important. A statistical-mechanical theory for confined molecular liquids provides a useful guide to the control that can be achieved by manipulating the affinity of electrode surfaces for water and varying the ion size.

The important point is that when d_- (size of platinum complex ions) is large enough, there is a physical factor excluding the anions from the bulk to the surface. This factor becomes stronger as d_- increases. Moreover, the strength is extremely sensitive to d_- . When the surface is hydrophobic, this factor dominates with the result that the anion concentration remains enriched in the immediate vicinity of the surface. For a pore having the size of a nanometer, the enrichment is kept remarkable within the whole nanospace. Thus, by modifying the silicon surface to make it hydrophobic and using platinum complex ions with considerably large d_- , we have succeeded in promoting electrodeposition within pores which are deep and extremely small in diameter. Without the physical factor, the reaction within such pores would be decelerated to a remarkable extent after a short time due to a diffusion-limited condition reached. Even when a pore is considerably large in diameter and the enrichment occurs only in the immediate vicinity of the pore surface, the continuous supply of reactants into the pore could be driven by *surface diffusion* arising from the concentration gradient formed along the surface. Once sufficiently large nuclei of platinum are formed on the electrode surface, the electrodeposition proceeds quite easily. The surface-induced structure could affect the electrostatic-potential profile across the electrode-solution interface during the electrodeposition which is important in understanding and controlling the electrochemical reaction. This issue is to be pursued in a future study.

To date, a variety of porous structures and solvents have been utilized in many applications. The present Letter, which has shown that the solvation properties of reactants in solvent confined on the scale of a nanometer play crucially important roles, sheds new light on design and control of highly efficient, chemical systems in a nanospace combined with proper solvents and reactants.

Acknowledgments

We thank Profs. K. Krischer (TU München) and S. Nakanishi (Univ. of Tokyo) for useful comments and suggestions. This Letter was supported by Grant-in-Aid for Young Scientists (B) (No. 23750239) and that for Scientific Research on Innovative Areas (No. 20118004) from MEXT.

Appendix A. Supplementary data

Supplementary data associated with this article can be found, in the online version, at <http://dx.doi.org/10.1016/j.cplett.2012.05.078>.

References

- [1] T.S. Koblenz, J. Wassenaar, J.N. Reek, *Chem. Soc. Rev.* 37 (2008) 247.
- [2] K. Kurotobi, Y. Murata, *Science* 333 (2011) 613.
- [3] Y.-W. Huang, Y.-C. Lai, C.-J. Tsai, Y.-W. Chiang, *Proc. Natl. Acad. Sci. USA* 108 (2011) 14145.
- [4] S. Han, M.Y. Choi, P. Kumar, H.E. Stanley, *Nat. Phys.* 6 (2010) 685.
- [5] Y. Zhang et al., *Proc. Natl. Acad. Sci. USA* 108 (2011) 12206.
- [6] V. Garcia-Morales, K. Krischer, *Proc. Natl. Acad. Sci. USA* 107 (2010) 4528.
- [7] V. Garcia-Morales, K. Krischer, *Proc. Natl. Acad. Sci. USA* 108 (2011) 19535.
- [8] R.M. Lynden-Bell, A.I. Frolov, M.V. Fedorov, *Phys. Chem. Chem. Phys.* 14 (2012) 2693.
- [9] A.I. Frolov, K. Kirchner, T. Kirchner, M.V. Fedorov, *Faraday Discuss.* 154 (2012) 154.
- [10] A.I. Frolov, R.N. Arif, M. Kolar, A.O. Romanova, M.V. Fedorov, A.G. Rozhin, *Chem. Sci.* 3 (2012) 541.
- [11] A. Imanishi, S. Yamane, Y. Nakato, *Langmuir* 24 (2008) 10755.
- [12] P.G. Kusalik, G.N. Patey, *J. Chem. Phys.* 88 (1988) 7715.
- [13] M. Kinoshita, S. Iba, M. Harada, *J. Chem. Phys.* 105 (1996) 2487.
- [14] M. Kinoshita, D.R. Bérard, *J. Comput. Phys.* 124 (1996) 230.
- [15] M. Kinoshita, *Condens. Matter. Phys.* 10 (2007) 387.
- [16] N.M. Cann, G.N. Patey, *J. Chem. Phys.* 106 (1997) 8165.
- [17] D.R. Bérard, M. Kinoshita, N.M. Cann, G.N. Patey, *J. Chem. Phys.* 107 (1997) 4719.
- [18] M. Kinoshita, M. Harada, *Mol. Phys.* 81 (1994) 1473.
- [19] J.C. Shelley, G.N. Patey, D.R. Bérard, G.M. Torrie, *J. Chem. Phys.* 107 (1997) 2122.
- [20] C.-Y. Lee, J.A. McCammon, P.J. Rossky, *J. Chem. Phys.* 80 (1984) 4448.
- [21] M. Kinoshita, F. Hirata, *J. Chem. Phys.* 106 (1997) 5202.